



HAL
open science

**Evaluated kinetic and photochemical data for
atmospheric chemistry: volume VIII – gas-phase
reactions of organic species with four, or more, carbon
atoms ($\geq C_4$)**

Abdelwahid Mellouki, Markus Ammann, R. Anthony Cox, John Crowley,
Hartmut Herrmann, Michael Jenkin, V. Faye Mcneill, Jürgen Troe, Timothy
Wallington

► **To cite this version:**

Abdelwahid Mellouki, Markus Ammann, R. Anthony Cox, John Crowley, Hartmut Herrmann, et al.. Evaluated kinetic and photochemical data for atmospheric chemistry: volume VIII – gas-phase reactions of organic species with four, or more, carbon atoms ($\geq C_4$). Atmospheric Chemistry and Physics, 2021, 21 (6), pp.4797-4808. 10.5194/ACP-21-4797-2021 . hal-03369753

HAL Id: hal-03369753

<https://hal.science/hal-03369753>

Submitted on 7 Oct 2021

HAL is a multi-disciplinary open access archive for the deposit and dissemination of scientific research documents, whether they are published or not. The documents may come from teaching and research institutions in France or abroad, or from public or private research centers.

L'archive ouverte pluridisciplinaire **HAL**, est destinée au dépôt et à la diffusion de documents scientifiques de niveau recherche, publiés ou non, émanant des établissements d'enseignement et de recherche français ou étrangers, des laboratoires publics ou privés.



Evaluated kinetic and photochemical data for atmospheric chemistry: volume VIII – gas-phase reactions of organic species with four, or more, carbon atoms ($\geq C_4$)

Abdelwahid Mellouki¹, Markus Ammann², R. Anthony Cox³, John N. Crowley⁴, Hartmut Herrmann⁵, Michael E. Jenkin⁶, V. Faye McNeill⁷, Jürgen Troe^{8,9}, and Timothy J. Wallington¹⁰

¹ICARE-CNRS, 1 C Av. de la Recherche Scientifique, 45071 Orléans CEDEX 2, France

²Laboratory of Environmental Chemistry, Paul Scherrer Institut, 5232 Villigen, Switzerland

³Centre for Atmospheric Science, Dept. of Chemistry, University of Cambridge, Lensfield Road, Cambridge, CB2 1EP, UK

⁴Max Planck Institute for Chemistry, Division of Atmospheric Chemistry, 55128 Mainz, Germany

⁵Atmospheric Chemistry Dept. (ACD), Leibniz Institute for Tropospheric Research (TROPOS), 04318 Leipzig, Germany

⁶Atmospheric Chemistry Services, Okehampton, Devon, EX20 4QB, UK

⁷Department of Chemical Engineering, Columbia University, New York, NY 10027, USA

⁸Max Planck Institute for Biophysical Chemistry, Am Fassberg 11, 37077 Göttingen, Germany

⁹Institute for Physical Chemistry, University of Göttingen, Tammannstr. 6, 37077 Göttingen, Germany

¹⁰Ford Motor Company, Research and Advanced Engineering, Mail Drop RIC-2122, Dearborn, Michigan 48121-2053, USA

Correspondence: Abdelwahid Mellouki (mellouki@cnrs-orleans.fr)

Received: 8 September 2020 – Discussion started: 16 September 2020

Revised: 8 February 2021 – Accepted: 8 February 2021 – Published: 29 March 2021

Abstract. This article, the eighth in the series, presents kinetic and photochemical data sheets evaluated by the IUPAC Task Group on Atmospheric Chemical Kinetic Data Evaluation. It covers the gas-phase thermal and photochemical reactions of organic species with four, or more, carbon atoms ($\geq C_4$) available on the IUPAC website in 2021, including thermal reactions of closed-shell organic species with HO and NO₃ radicals and their photolysis. The present work is a continuation of volume II (Atkinson et al., 2006), with new reactions and updated data sheets for reactions of HO (77 reactions) and NO₃ (36 reactions) with $\geq C_4$ organics, including alkanes, alkenes, dienes, aromatics, oxygenated, organic nitrates and nitro compounds in addition to photochemical processes for nine species. The article consists of a summary table (Table 1), containing the recommended kinetic parameters for the evaluated reactions, and a supplement containing the data sheets, which provide information upon which recommendations are made.

1 Introduction

In the mid-1970s, it was appreciated that there was a need for the establishment of an international panel to produce a set of critically evaluated rate parameters for reactions of interest for atmospheric chemistry. To this end, the CODATA Task Group on Chemical Kinetics, under the auspices of the International Council of Scientific Unions (ICSU), was formed in 1977 and tasked to produce an evaluation of relevant, available kinetic and photochemical data. The first evaluation by this international committee was published in *J. Phys. Chem. Ref. Data* in 1980 (Baulch et al., 1980), followed by supplements in 1982 (Baulch et al., 1982) and 1984 (Baulch et al., 1984). In 1986 the IUPAC Subcommittee on Gas Kinetic Data Evaluation for Atmospheric Chemistry superseded the original CODATA Task Group for Atmospheric Chemistry. The subcommittee continued its data evaluation programme with supplements published in 1989 (Atkinson et al., 1989), 1992 (Atkinson et al., 1992), 1997 (Atkinson et al., 1997a), 1997 (Atkinson et al., 1997b), 1999 (Atkinson et al., 1999) and 2000 (Atkinson et al., 2000).

The gas-phase evaluation work was expanded to include heterogeneous reactions of gases on solid and liquid substrates in 2005. Aqueous-phase reactions of atmospheric importance were added in 2015. The IUPAC group's work now includes over 1400 gas-phase, heterogeneous and aqueous-phase reactions of importance in atmospheric chemistry. Reflecting the broader scope, the group changed its name to the IUPAC Task Group on Atmospheric Chemical Kinetic Data Evaluation in 2013. Cox (2012) and Cox et al. (2018) discuss the history of IUPAC data evaluations and their role in addressing the critical societal challenges of stratospheric ozone loss, tropospheric ozone formation, acid rain, urban air pollution, aerosol formation and climate change.

In 2000 the evaluation was made available on the World Wide Web (<http://iupac.pole-ether.fr>, last access: 25 January 2021). The IUPAC website hosts an interactive database with a search facility and hyperlinks between the summary table and the data sheets, both of which can be downloaded as individual Word and PDF files. Work is underway to convert the data sheets to machine-readable XML files, which will enable the automatic transfer of IUPAC-recommended data into atmospheric models. The IUPAC group continues to update and extend the set of evaluated reactions. To enhance the accessibility of this updated material to the scientific community, the evaluation has been published as a series of articles in *Atmospheric Chemistry and Physics* (Atkinson et al., 2004, 2006, 2007, 2008; Crowley et al., 2010; Ammann et al., 2013; Cox et al., 2020). We present here in volume VIII new data sheets for gas-phase thermal and photochemical initiation reactions of organic species with four, or more, carbon atoms. The coverage of this volume includes evaluation of the thermal reactions of the organic species with HO and NO₃ radicals and photolysis. The reactions with O₃ are included in a separate volume within this series (Cox et al., 2020), along with the chemistry of the Criegee intermediates produced. The coverage of the evaluation was previously limited to the reactions of $\leq C_3$ organics, selected larger species (*n*-butane, isoprene, 2-methyl-but-3-en-2-ol and α -pinene) and some related oxygenated products (Atkinson et al., 2006). This has been substantially increased to include all C₄ alkanes and alkenes, benzene and toluene, monoterpenes and sesquiterpenes and related oxygenated products. This volume therefore presents evaluations for 97 new reactions and updates for 25 reactions of organic species with four, or more, carbon atoms.

2 Guide to the data sheets

For each reaction covered in this volume, a data sheet with details about, for example, experimental methods and a justification of the choice of preferred value is available in the Supplement. The data sheets covering gas-phase reactions are principally of two types: (i) those for individual thermal

reactions and (ii) those for the individual photochemical reactions.

2.1 Thermal reactions

The data sheets begin with a statement of the reactions including known/potential product channels when this information is available. The available kinetic data on the reactions are summarized under two headings: (i) absolute rate coefficients and (ii) relative rate coefficients. Under both headings, we list the published experimental data as absolute rate coefficients. If the temperature coefficient has been measured, the results are given in a temperature-dependent form over a stated temperature range. For bimolecular reactions, the temperature dependence is usually expressed in the normal Arrhenius form, $k = A \exp(-B/T)$, where $B = E/R$. For a few bimolecular reactions, we have listed temperature dependencies in alternative forms such as $k = C(T/298 \text{ K})^n \exp(-D/T)$ or $k = ET^2 \exp(-F/T)$, where the original authors have found that alternative expressions give a better fit to the data. In our recommendations we seek to provide simple Arrhenius expressions that describe the kinetics over the atmospherically relevant temperature range (200–300 K). More complex expressions which are often needed to describe the kinetic behaviour over larger ranges of temperature are given in the “Comments on preferred values” section in the data sheets. Rate coefficients are given here in units of cubic centimetres per molecule per second ($\text{cm}^3 \text{ molecule}^{-1} \text{ s}^{-1}$). Note that “molecule” is not a unit recognized by IUPAC but is included for clarity. For pressure-dependent combination and dissociation reactions, the non-Arrhenius temperature dependence is used. This is discussed more fully in a subsequent section of this guide. Single temperature data are presented as such, and wherever possible the rate coefficient at, or close to, 298 K is quoted directly as measured by the original authors. This means that the listed rate coefficient at 298 K may differ slightly from that calculated from the Arrhenius parameters determined by the same authors. Rate coefficients at 298 K marked with an asterisk indicate that the value was calculated by extrapolation of a measured temperature range which did not include 298 K. The tables of experimental data are supplemented by a series of comments summarizing the experimental details. The abbreviations relating to experimental techniques that are used in the “Techniques/comments” and “Comments” sections are defined in the Appendix.

For measurements of relative rate coefficients, wherever possible the comments contain the actual measured ratio of rate coefficients together with the rate coefficient of the reference reaction used to calculate the absolute rate coefficient listed in the data table. The absolute value of the rate coefficient given in the table may be different from that reported by the original author, owing to a different choice of rate coefficient of the reference reaction. Whenever possible the ref-

Table 1. Summary of recommended rate coefficients for organic ($\geq C_4$) reactions.

Reaction number	Reaction	k_{298} ($\text{cm}^3 \text{ molecule}^{-1} \text{ s}^{-1}$)	$\Delta \log k_{298}^*$	Temp. dependence of k ($\text{cm}^3 \text{ molecule}^{-1} \text{ s}^{-1}$)	Temp. range (K)	$\Delta (E/R)$ (K)*
HO reactions based on data sheets in the Supplement and on the IUPAC website updated in 2019						
HOx_VOC7	HO + <i>n</i> -butane \rightarrow H ₂ O + CH ₂ CH ₂ CH ₂ CH ₃ \rightarrow H ₂ O + CH ₃ CHCH ₂ CH ₃					
	Overall	2.35×10^{-12}	± 0.06	$9.8 \times 10^{-12} \exp(-425/T)$	180–300	± 100
HOx_VOC8	HO + isoprene \rightarrow products	1.0×10^{-10}	± 0.06	$2.1 \times 10^{-11} \exp(465/T)$	240–630	± 150
HOx_VOC9	HO + α -pinene \rightarrow products	5.3×10^{-11}	± 0.08	$1.3 \times 10^{-11} \exp(410/T)$	240–360	± 100
HOx_VOC14	HO + <i>n</i> -butanal \rightarrow products	2.3×10^{-11}	± 0.08	$5.8 \times 10^{-12} \exp(410/T)$	250–430	± 250
HOx_VOC15	HO + methacrolein \rightarrow products	3.0×10^{-11}	± 0.08	$8.4 \times 10^{-12} \exp(380/T)$	230–380	± 100
HOx_VOC20	HO + 2-butanone \rightarrow products	1.1×10^{-12}	± 0.10	$1.5 \times 10^{-12} \exp(-90/T)$	210–300	± 200
HOx_VOC21	HO + methyl vinyl ketone \rightarrow products	2.0×10^{-11}	± 0.10	$2.6 \times 10^{-12} \exp(610/T)$	230–380	± 200
HOx_VOC22	HO + pinonaldehyde \rightarrow products	3.9×10^{-11}	± 0.15	$5.2 \times 10^{-12} \exp(600/T)$	230–380	± 300
HOx_VOC27	HO + 1-butanol \rightarrow products	8.5×10^{-12}	± 0.06	$5.3 \times 10^{-12} \exp(140/T)$	260–380	± 200
HOx_VOC28	HO + 2-butanol \rightarrow products	8.7×10^{-12}	± 0.08			
HOx_VOC29	HO + 2-methyl-3-buten-2-ol \rightarrow products	6.3×10^{-11}	± 0.08	$8.1 \times 10^{-12} \exp(610/T)$	230–300	± 200
HOx_VOC31	HO + 3-methylfuran \rightarrow products	9.3×10^{-11}	± 0.15			
HOx_VOC33	HO + 2-hydroxy-2-methylpropanal \rightarrow products	1.4×10^{-11}	± 0.10			
HOx_VOC42	HO + 1-butyl nitrate \rightarrow products	1.6×10^{-12}	± 0.06			
HOx_VOC43	HO + 2-butyl nitrate \rightarrow products	8.6×10^{-13}	± 0.15			
HOx_VOC46	HO + 1-nitrooxy-2-butanone \rightarrow products	8.2×10^{-13}	± 0.30			
HOx_VOC47	HO + 3-nitrooxy-2-butanone \rightarrow products	1.2×10^{-12}	± 0.30			
HOx_VOC48	HO + 2-methyl-1-(nitroperoxy)-2-propen-1-one \rightarrow products	2.9×10^{-11}	$+0.2$ -0.5			
HOx_VOC60	HO + 2-methylpropane \rightarrow H ₂ O + (CH ₃) ₃ C \rightarrow H ₂ O + (CH ₃) ₂ CHCH ₂					
	Overall	2.1×10^{-12}	± 0.04	$5.4 \times 10^{-12} \exp(-285/T)$	210–300	± 150
HOx_VOC61	HO + 2-methylpropene \rightarrow products	5.1×10^{-11}	± 0.04	$9.4 \times 10^{-12} \exp(505/T)$	290–430	± 200
HOx_VOC62	HO + 1-butene \rightarrow products	3.1×10^{-11}	± 0.06	$6.6 \times 10^{-12} \exp(465/T)$	290–430	± 150
HOx_VOC63	HO + <i>cis</i> -2-butene \rightarrow products	5.6×10^{-11}	± 0.10	$1.1 \times 10^{-11} \exp(485/T)$	290–430	± 200
HOx_VOC64	HO + <i>trans</i> -2-butene \rightarrow products	7.1×10^{-11}	± 0.06	$1.1 \times 10^{-11} \exp(553/T)$	290–430	± 200
HOx_VOC66	HO + biacetyl \rightarrow products	2.3×10^{-13}	± 0.06	$5.25 \times 10^{-13} \exp(-243/T)$	240–350	± 50
HOx_VOC67	HO + <i>n</i> -butanoic acid \rightarrow products	1.8×10^{-12}	± 0.15			
HOx_VOC68	HO + <i>i</i> -butanal \rightarrow products	2.6×10^{-11}	± 0.04	$6.8 \times 10^{-12} \exp(410/T)$	240–425	± 60
HOx_VOC69	HO + 2-methyl-1-propanol \rightarrow products	8.9×10^{-12}	± 0.08	$2.73 \times 10^{-12} \exp(352/T)$	240–370	± 120
HOx_VOC70	HO + 2-methyl-2-propanol \rightarrow products	1.1×10^{-12}	± 0.06	$1.6 \times 10^{-12} \exp(-121/T)$	240–314	± 75
HOx_VOC76	HO + 2-hydroxybutanal \rightarrow C ₂ H ₅ CH(OH)CO + H ₂ O \rightarrow C ₂ H ₅ C(OH)CHO + H ₂ O					
	Overall	2.4×10^{-11}	± 0.10			
HOx_VOC77	HO + 1-nitrooxy-2-butanol \rightarrow products	7.0×10^{-12}	± 0.20			
HOx_VOC78	HO + 2-nitrooxy-1-butanol \rightarrow products	7.4×10^{-12}	± 0.20			
HOx_VOC79	HO + 3-hydroxy-2-butanone \rightarrow H ₂ O + CH ₃ C(O)C(OH)CH ₃ \rightarrow products					
	Overall	9.7×10^{-12}	± 0.10	$1.24 \times 10^{-12} \exp(612/T)$	280–350	± 350
HOx_VOC84	HO + α -terpinene \rightarrow products	3.5×10^{-10}	± 0.08			
HOx_VOC85	HO + γ -terpinene \rightarrow products	1.7×10^{-10}	± 0.10			
HOx_VOC86	HO + terpinolene \rightarrow products	2.2×10^{-10}	± 0.15			
HOx_VOC87	HO + α -phellandrene \rightarrow products	3.2×10^{-10}	± 0.08			
HOx_VOC88	HO + β -phellandrene \rightarrow products	1.7×10^{-10}	± 0.15			
HOx_VOC89	HO + α -cedrene \rightarrow products	6.7×10^{-11}	± 0.10			
HOx_VOC90	HO + longifolene \rightarrow products	4.7×10^{-11}	± 0.10			
HOx_VOC91	HO + α -copaene \rightarrow products	9.0×10^{-11}	± 0.10			
HOx_VOC92	HO + β -caryophyllene \rightarrow products	2.0×10^{-10}	± 0.15			
HOx_VOC93	HO + α -humulene \rightarrow products	2.9×10^{-10}	± 0.10			
HOx_VOC99	HO + β -pinene \rightarrow products	7.6×10^{-11}	± 0.05	$1.62 \times 10^{-11} \exp(460/T)$	240–420	± 150
HOx_VOC100	HO + limonene \rightarrow products	1.65×10^{-10}	± 0.05	$3.41 \times 10^{-11} \exp(470/T)$	220–360	± 150
HOx_VOC101	HO + camphene \rightarrow products	5.2×10^{-11}	± 0.10	$4.14 \times 10^{-12} \exp(754/T)$	280–320	± 100
HOx_VOC102	HO + 2-carene \rightarrow products	8.0×10^{-11}	± 0.15			
HOx_VOC103	HO + 3-carene \rightarrow products	8.3×10^{-11}	± 0.06	$2.5 \times 10^{-11} \exp(357/T)$	230–360	± 50
HOx_VOC104	HO + β -myrcene \rightarrow products	2.1×10^{-10}	± 0.15			
HOx_VOC105	HO + β -ocimene \rightarrow products	2.8×10^{-10}	± 0.15	$4.0 \times 10^{-11} \exp(579/T)$	310–430	± 150
HOx_VOC106	HO + β -sabinene \rightarrow products	1.2×10^{-10}	± 0.15			
HOx_VOC107	HO + α -farnesene \rightarrow products	2.2×10^{-10}	± 0.30	2.2×10^{-10}	298–430	± 200
HOx_VOC108	HO + β -farnesene \rightarrow products	2.3×10^{-10}	± 0.30	2.3×10^{-10}	298–430	± 200
HOx_VOC109	HO + α -terpinol \rightarrow products	1.9×10^{-10}	± 0.30			
HOx_AROM1	HO + benzene \rightarrow H ₂ O + C ₆ H ₅ \rightarrow HOC ₆ H ₆	8×10^{-15}	± 0.50	$3.8 \times 10^{-11} \exp(-2520/T)$	330–1410	± 300
	Overall	1.2×10^{-12}	± 0.06	$2.3 \times 10^{-12} \exp(-190/T)$	230–350	± 200

Table 1. Continued.

Reaction number	Reaction	k_{298} ($\text{cm}^3 \text{ molecule}^{-1} \text{ s}^{-1}$)	$\Delta \log k_{298}^*$	Temp. dependence of k ($\text{cm}^3 \text{ molecule}^{-1} \text{ s}^{-1}$)	Temp. range (K)	$\Delta (E/R)$ (K)*
HOx_AROM2	HO + toluene \rightarrow H ₂ O + C ₆ H ₅ CH ₂ \rightarrow HOC ₆ H ₅ CH ₃	3.5×10^{-13}	± 0.20	$2.5 \times 10^{-11} \exp(-1270/T)$	310–1050	± 200
	Overall	5.6×10^{-12}	± 0.06	$1.8 \times 10^{-12} \exp(340/T)$	210–350	± 200
HOx_AROM3	HO + <i>m</i> -cresol \rightarrow H ₂ O + CH ₃ C ₆ H ₄ O \rightarrow H ₂ O + CH ₂ C ₆ H ₄ OH \rightarrow CH ₃ C ₆ H ₄ (OH) ₂					
	Overall	6.2×10^{-11}	± 0.10	$2.4 \times 10^{-12} \exp(965/T)$	290–350	± 600
HOx_AROM4	HO + <i>o</i> -cresol \rightarrow H ₂ O + CH ₃ C ₆ H ₄ O \rightarrow H ₂ O + CH ₂ C ₆ H ₄ OH \rightarrow CH ₃ C ₆ H ₄ (OH) ₂					
	Overall	4.2×10^{-11}	± 0.10	$1.6 \times 10^{-12} \exp(970/T)$	290–350	± 600
HOx_AROM5	HO + <i>p</i> -cresol \rightarrow H ₂ O + CH ₃ C ₆ H ₄ O \rightarrow H ₂ O + CH ₂ C ₆ H ₄ OH \rightarrow CH ₃ C ₆ H ₄ (OH) ₂					
	Overall	4.8×10^{-11}	± 0.10	$1.9 \times 10^{-12} \exp(970/T)$	290–350	± 600
HOx_AROM6	HO + phenol \rightarrow H ₂ O + C ₆ H ₅ O \rightarrow H ₂ O + C ₆ H ₄ OH \rightarrow HOC ₆ H ₅ OH					
	Overall	2.8×10^{-11}	± 0.08	$4.7 \times 10^{-13} \exp(1220/T)$	290–350	± 600
HOx_AROM7	HO + 1,2-dihydroxybenzene \rightarrow products	1.0×10^{-10}	± 0.15			
HOx_AROM8	HO + 1,2-dihydroxy-3-methylbenzene \rightarrow products	2.0×10^{-10}	± 0.15			
HOx_AROM9	HO + 1,2-dihydroxy-4-methylbenzene \rightarrow products	1.5×10^{-10}	± 0.15			
HOx_AROM10	HO + 3-methyl-2-nitrophenol \rightarrow products	3.4×10^{-12}	± 0.30			
HOx_AROM11	HO + 4-methyl-2-nitrophenol \rightarrow products	3.4×10^{-12}	± 0.15			
HOx_AROM12	HO + 5-methyl-2-nitrophenol \rightarrow products	6.4×10^{-12}	± 0.20			
HOx_AROM13	HO + 6-methyl-2-nitrophenol \rightarrow products	2.5×10^{-12}	± 0.30			
HOx_AROM14	HO + 1,4-benzoquinone \rightarrow products	4.6×10^{-12}	± 0.15			
HOx_AROM15	HO + methyl-1,4-benzoquinone \rightarrow products	2.3×10^{-11}	± 0.15			
HOx_AROM16	HO + nitrobenzene \rightarrow products	1.4×10^{-13}	± 0.20	$6.0 \times 10^{-13} \exp(-440/T)$	250–370	± 300
HOx_AROM17	HO + 3-nitrotoluene \rightarrow products	1.2×10^{-12}	± 0.50			
HOx_AROM18	HO + <i>cis</i> -but-2-enedial \rightarrow products	5.7×10^{-11}	± 0.20			
HOx_AROM19	HO + <i>trans</i> -but-2-enedial \rightarrow products	$\geq 2 \times 10^{-11}$				
HOx_AROM20	HO + 3 <i>H</i> -furan-2-one \rightarrow products	4.8×10^{-11}	± 0.20			
HOx_AROM21	HO + furan-2,5-dione \rightarrow products	1.4×10^{-12}	± 0.20			
HOx_AROM22	HO + <i>cis/trans</i> -4-oxopent-2-enal \rightarrow products	6.2×10^{-11}	± 0.20			
HOx_AROM25	HO + benzaldehyde \rightarrow products	1.26×10^{-11}	± 0.08	$5.9 \times 10^{-12} \exp(225/T)$	290–350	± 170
HOx_AROM26	HO + benzyl alcohol \rightarrow products	2.7×10^{-11}	± 0.08			
NO ₃ reactions based on data sheets in the Supplement and on the IUPAC website updated in 2019						
NO3_VOC26	NO ₃ + 2-methylpropane \rightarrow products	1.1×10^{-16}	± 0.10	$3.0 \times 10^{-12} \exp(-3050/T)$	290–430	± 300
NO3_VOC27	NO ₃ + 2-methylpropene \rightarrow products	3.4×10^{-13}	± 0.10			
NO3_VOC28	NO ₃ + 1-butene \rightarrow products	1.3×10^{-14}	± 0.10	$3.2 \times 10^{-13} \exp(-950/T)$	230–480	± 200
NO3_VOC29	NO ₃ + <i>cis</i> -2-butene \rightarrow products	3.5×10^{-13}	± 0.10			
NO3_VOC30	NO ₃ + <i>trans</i> -2-butene \rightarrow products	3.9×10^{-13}	± 0.08	$\{1.78 \times 10^{-12} \exp(-530/T)$ $+ 1.28 \times 10^{-14} \exp(570/T)\}$	200–380	
NO3_VOC33	NO ₃ + <i>d</i> -limonene \rightarrow products	1.2×10^{-11}	± 0.12			
NO3_VOC34	NO ₃ + 2-carene \rightarrow products	2.0×10^{-11}	± 0.12			
NO3_VOC35	NO ₃ + 3-carene \rightarrow products	9.1×10^{-12}	± 0.12			
NO3_VOC36	NO ₃ + β -pinene \rightarrow products	2.5×10^{-12}	± 0.12			
NO3_VOC37	NO ₃ + myrcene \rightarrow products	1.1×10^{-11}	± 0.12			
NO3_VOC38	NO ₃ + sabinene \rightarrow products	1.0×10^{-11}	± 0.10			
NO3_VOC39	NO ₃ + ocimene, <i>cis</i> and <i>trans</i> \rightarrow products	2.2×10^{-11}	± 0.15			
NO3_VOC40	NO ₃ + α -terpinene \rightarrow products	1.8×10^{-10}	± 0.25			
NO3_VOC41	NO ₃ + γ -terpinene \rightarrow products	2.9×10^{-11}	± 0.12			
NO3_VOC42	NO ₃ + α -phellandrene \rightarrow products	7.3×10^{-11}	± 0.15			
NO3_VOC43	NO ₃ + terpinolene \rightarrow products	9.7×10^{-11}	± 0.25			
NO3_VOC46	NO ₃ + camphene \rightarrow products	6.6×10^{-13}	± 0.10			
NO3_VOC47	NO ₃ + β -caryophyllene \rightarrow products	1.9×10^{-11}	± 0.25			
NO3_VOC48	NO ₃ + α -cedrene \rightarrow products	8.2×10^{-12}	± 0.25			
NO3_VOC49	NO ₃ + α -humulene \rightarrow products	3.5×10^{-11}	± 0.25			
NO3_VOC50	NO ₃ + α -copaene \rightarrow products	1.6×10^{-11}	± 0.25			
NO3_VOC51	NO ₃ + longifolene \rightarrow products	6.8×10^{-13}	± 0.25			
NO3_VOC52	NO ₃ + isolongifolene \rightarrow products	3.9×10^{-12}	± 0.25			
NO3_VOC53	NO ₃ + alloisolongifolene \rightarrow products	1.4×10^{-12}	± 0.25			
NO3_VOC54	NO ₃ + α -neoclovene \rightarrow products	8.25×10^{-12}	± 0.25			
NO3_VOC55	NO ₃ + valencene \rightarrow products	7.9×10^{-12}	± 0.25			
NO3_VOC56	NO ₃ + α -terpineol \rightarrow products	1.7×10^{-11}	± 0.25			
NO3_AROM1	NO ₃ + benzene \rightarrow products	$< 3 \times 10^{-17}$				
NO3_AROM2	NO ₃ + toluene \rightarrow products	7.8×10^{-17}	± 0.25			
NO3_AROM3	NO ₃ + <i>m</i> -cresol \rightarrow CH ₃ C ₆ H ₄ O + HNO ₃ \rightarrow other products					

Table 1. Continued.

Reaction number	Reaction	k_{298} ($\text{cm}^3 \text{ molecule}^{-1} \text{ s}^{-1}$)	$\Delta \log k_{298}^*$	Temp. dependence of k ($\text{cm}^3 \text{ molecule}^{-1} \text{ s}^{-1}$)	Temp. range (K)	$\Delta (E/R)$ (K)*
	Overall	1.0×10^{-11}	± 0.15			
NO3_AROM4	$\text{NO}_3 + o\text{-cresol} \rightarrow \text{CH}_3\text{C}_6\text{H}_4\text{O} + \text{HNO}_3$ \rightarrow other products					
	Overall	1.4×10^{-11}	± 0.15			
NO3_AROM5	$\text{NO}_3 + p\text{-cresol} \rightarrow \text{CH}_3\text{C}_6\text{H}_4\text{O} + \text{HNO}_3$ \rightarrow other products					
	Overall	1.1×10^{-11}	± 0.15			
NO3_AROM6	$\text{NO}_3 + \text{phenol} \rightarrow \text{C}_6\text{H}_5\text{O} + \text{HNO}_3$ \rightarrow other products					
	Overall	3.8×10^{-12}	± 0.15			
NO3_AROM7	$\text{NO}_3 + 1,2\text{-dihydroxybenzene} \rightarrow$ products	9.9×10^{-11}	± 0.15			
NO3_AROM8	$\text{NO}_3 + 1,2\text{-dihydroxy-3-methylbenzene} \rightarrow$ products	1.7×10^{-10}	± 0.15			
NO3_AROM9	$\text{NO}_3 + 1,2\text{-dihydroxy-4-methylbenzene} \rightarrow$ products	1.5×10^{-10}	± 0.15			
Photochemical reactions based on data sheets in the Supplement and on the IUPAC website updated in 2019						
P8	butanone $+h\nu \rightarrow$ products					
P23	biacetyl $+h\nu \rightarrow$ products					
P24	<i>i</i> -butyraldehyde $+h\nu \rightarrow$ products					
P26	<i>cis-trans</i> -but-2-enedial $+h\nu \rightarrow$ products					
P27	4-oxopent-2-enal $+h\nu \rightarrow$ products					
P28	2-nitrophenol $+h\nu \rightarrow$ products					
P30	benzaldehyde $+h\nu \rightarrow$ products					
P31	3-methyl-2-nitrophenol $+h\nu \rightarrow$ products					
P32	4-methyl-2-nitrophenol $+h\nu \rightarrow$ products					

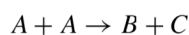
* The cited uncertainty corresponds approximately to 95 % confidence limits.

erence rate coefficient data are those preferred in the present evaluation.

The preferred values in the data sheets are based on our consideration of the suitability of the experimental method and coverage of applicable parameter space (temperature, total pressure of diluent gas, partial pressure of gas-phase species) within the atmospherically relevant range. The general approach and methods used have been reviewed by Cox (2012). It is recognized that preferred values may change with publication of new data, and such changes are updated on the website. The preferred rate coefficients are presented (i) at a temperature of 298 K and (ii) in temperature-dependent form over a stated temperature range. This is followed by a statement of the uncertainty limits in $\log k$ at 298 K and the uncertainty limits in (E/R) , for the mean temperature in the range. Some comments on the assignment of uncertainties are given later in this guide to the data sheets. The ‘‘Comments on preferred values’’ describe how the selection was made and give any other relevant information. The extent of the comments depends upon the present state of our knowledge of the particular reaction in question. The data sheets are concluded with a list of the relevant references.

2.2 Conventions concerning rate coefficients

All of the reactions are considered to be elementary processes. Thus the rate expression is derived from a statement of the reaction, e.g.

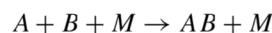


$$-\frac{1}{2} \frac{d[A]}{dt} = \frac{d[B]}{dt} = \frac{d[C]}{dt} = k[A]^2. \quad (1)$$

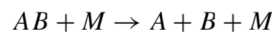
Note that the stoichiometric coefficient for A, i.e. 2, appears in the denominator before the rate of change of [A] (which is equal to $2k[A]^2$) and as a power on the right-hand side. Representations of k as a function of temperature characterize simple ‘‘direct’’ bimolecular reactions. Sometimes it is found that k also depends on the pressure and the nature of the bath gas. This may be an indication of complex formation during the course of the bimolecular reaction, which is always the case in combination reactions. In the following sections the representations of k which are adopted in these cases are explained.

2.3 Treatment of combination and dissociation reactions

Unlike simple bimolecular reactions such as those considered in Sect. 2.2, combination reactions



and the reverse dissociation reactions



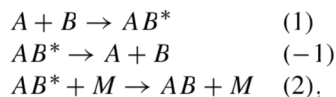
are composed of sequences of different types of physical and chemical elementary processes. Their rate coefficients reflect the more complicated sequential mechanism and depend on the temperature, T , and the nature and concentration of the third body, M . In this evaluation, the combination reactions are described by a formal second-order rate law:

$$\frac{d[AB]}{dt} = k[A][B], \quad (2)$$

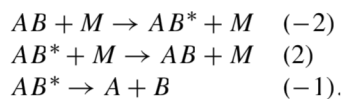
while dissociation reactions are described by a formal first-order rate law:

$$\frac{-d[AB]}{dt} = k[AB]. \quad (3)$$

In both cases, k depends on the temperature and on the concentration of M , i.e. $[M]$. To rationalize the representations of the rate coefficients used in this evaluation, we first consider the Lindemann–Hinshelwood reaction scheme. The combination reactions follow an elementary mechanism of the form



while the dissociation reactions are characterized by



Assuming quasi-stationary concentrations for the highly excited unstable species AB^* (i.e. that $d[AB^*]/dt \approx 0$), it follows that the rate coefficient for the combination reaction is given by

$$k = k_1 \left(\frac{k_2[M]}{k_{-1} + k_2[M]} \right), \quad (4)$$

while that for the dissociation reaction is given by

$$k = k_{-2}[M] \left(\frac{k_{-1}}{k_{-1} + k_2[M]} \right). \quad (5)$$

In these equations the expressions before the parentheses represent the rate coefficients of the process initiating the reaction, whereas the expressions within the parentheses denote the fraction of reaction events which, after initiation,

complete the reaction to products. In the low-pressure limit ($[M] \rightarrow 0$) the rate coefficients are proportional to $[M]$; in the high-pressure limit ($[M] \rightarrow \infty$) they are independent of $[M]$. It is useful to express k in terms of the limiting low-pressure and high-pressure rate coefficients:

$$\begin{aligned} k_0 &= \lim_{[M] \rightarrow 0} k([M]) \text{ for } [M] \rightarrow 0 \\ \text{and } k_\infty &= \lim_{[M] \rightarrow \infty} k([M]) \text{ for } [M] \rightarrow \infty. \end{aligned} \quad (6)$$

From this convention, the Lindemann–Hinshelwood equation is obtained:

$$k = \frac{k_0 k_\infty}{k_0 + k_\infty}. \quad (7)$$

It follows that, for combination reactions, $k_0 = k_1 k_2 [M] / k_{-1}$ and $k_\infty = k_1$, while, for dissociation reactions, $k_0 = k_{-2} [M]$ and $k_\infty = k_{-1} k_{-2} / k_2$. Since detailed balancing applies, the ratio of the rate coefficients for combination and dissociation at a fixed T and $[M]$ is given by the equilibrium constant $K_c = k_1 k_2 / k_{-1} k_{-2}$.

Starting from the high-pressure limit, the rate coefficients fall off with decreasing third-body concentration $[M]$, and the corresponding representation of k as a function of $[M]$ is termed the “falloff curve” of the reaction. In practice, the above Lindemann–Hinshelwood expressions do not suffice to characterize the falloff curves completely. Because of the multistep character of the collisional deactivation ($k_2[M]$) and activation ($k_{-2}[M]$) processes, and energy and angular momentum dependences of the association (k_1) and dissociation (k_{-1}) steps, as well as other phenomena, the falloff expressions have to be modified. This can be done by including a broadening factor F in the Lindemann–Hinshelwood expression (Troe, 1979):

$$k = \frac{k_0 k_\infty}{k_0 + k_\infty} F = k_0 \left(\frac{1}{1+x} \right) F = k_\infty \left(\frac{x}{1+x} \right) F. \quad (8)$$

The broadening factor F depends on the ratio $x = k_0/k_\infty$, which is proportional to $[M]$, and can be used as a measure of “reduced pressure”. The first factors on the right-hand side represent the Lindemann–Hinshelwood expression, and the additional broadening factor F , at not too high temperatures, is approximately given by (Troe, 1979)

$$\log F \cong \frac{\log F_c}{1 + [\log(k_0/k_\infty)/N]^2}, \quad (9)$$

where $\log = \log_{10}$ and $N \approx [0.75 - 1.27 \log F_c]$.

When F_c decreases, the falloff curve broadens and becomes asymmetric (i.e. $F(k_0/k_\infty) \neq F(k_\infty/k_0)$). The given equation for F then becomes insufficient and should be replaced, for example, by

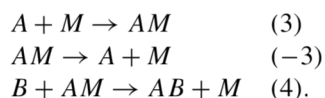
$$F(x) \approx (1+x)/(1+x^n)^{1/n}, \quad (10)$$

where $x = k_0/k_\infty$, $n = [\ln 2 / \ln(2/F_c)] [0.8 + 0.2 x^q]$, $q = (F_c - 1) / \ln(F_c/10)$ and $\ln = \log_e$ (Troe and Ushakov, 2014).

While the former equation for $\log F$ appears acceptable as long as $F_c \geq 0.6$, the latter equation for F should be used for $F_c \leq 0.6$. With these equations, falloff curves are represented in terms of the three parameters k_0 (being proportional to $[M]$), k_∞ and F_c .

The parameters k_0 , k_∞ and F_c depend on details of the intra- and intermolecular dynamics and in principle can be calculated. If the required information is not available, one has to obtain them by fitting experimental falloff curves with the expressions given above. Nevertheless, one may estimate F_c to be typically of the order of 0.49, 0.44, 0.39 and 0.35, if the reactants A and B in total have $r = 3, 4, 5$, and 6 external rotational degrees of freedom, respectively (Cobos and Troe, 2003; for the reaction $\text{HO} + \text{NO}_2 + M$, for example, one would have $r = 5$ and $F_c \approx 0.39$); F_c may be lower if low-frequency vibrations in A or B are relevant in addition to the rotations and if collisions are inefficient. Over the range 200–300 K, often one can neglect a temperature dependence of F_c (for detailed calculations of F_c , including a dependence on the bath gas M , see, for example, Troe 1983; Troe and Ushakov, 2011, 2014). The accuracy of $F(x)$ as given above is estimated to be about 10%. Larger differences between experimentally fitted F_c often are an indication of inadequate falloff extrapolations to k_0 and/or k_∞ . In this case, the apparent values for k_0 , k_∞ and F_c can still provide a satisfactory representation of the considered experimental data, in spite of the fact that k_0 and/or k_∞ are not the real limiting values. If falloff curves are fitted in different ways, changes in F_c require changes in the limiting k_0 and k_∞ . In the present evaluation, we generally follow the experimentally fitted values for k_0 , k_∞ and F_c , provided that F_c does not differ too much from the standard values given above and theoretically modelled values. If large deviations are encountered, the experimental data are re-evaluated using F_c values as given above. Values of k_∞ for combination reactions without a barrier often have only weak temperature dependences, which in practice can be neglected.

Besides the energy-transfer mechanism, i.e. Reactions (1), (–1), and (2), a second mechanism may become relevant for some reactions considered here. This is the radical-complex (or chaperon) mechanism,



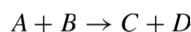
which, in the low-pressure range, leads to $k_0 = (k_3/k_{-3})k_4[M]$. For some tri- and tetra-atomic adducts AB , e.g. $\text{O} + \text{O}_2 \rightarrow \text{O}_3$ and $\text{HO} + \text{C}_6\text{H}_6 \rightarrow \text{HOC}_6\text{H}_6$, the value of k_0 may exceed that from the energy-transfer mechanism and show stronger temperature dependences (Luther et al., 2005; Teplukhin and Babikov, 2016). This mechanism may also influence high-pressure experiments when k_0 from the radical-complex mechanism exceeds k_∞ from the energy-transfer mechanism (Oum et al., 2003). In this case falloff over wide pressure ranges cannot be represented by contributions from

the energy-transfer mechanism alone, in particular when measurements at pressures above about 1×10^6 Pa are taken into consideration.

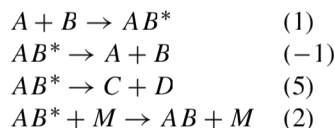
The dependence of k_0 and k_∞ on temperature T is represented in the form $k \propto T^{-n}$ except for cases with an established energy barrier in the potential. We have used this form of temperature dependence because it usually gives a better fit to the data over a wider range of temperature than the Arrhenius expression does. It should be emphasized that the chosen form of the temperature dependence is often only adequate over limited temperature ranges such as 200–300 K. Obviously, the relevant values of n are different for k_0 and k_∞ . In this evaluation, values of k_0 are given for selected examples of third bodies M , and if possible for $M = \text{N}_2, \text{O}_2$ or air.

2.4 Treatment of complex-forming bimolecular reactions

Bimolecular reactions may follow the “direct” pathway



and/or involve complex formation, in the simplest way characterized by the steps



(there may be additional pathways following from AB^* ; direct and complex-forming pathways may or may not be coupled). Assuming quasi-stationary concentrations of AB^* (i.e. that $d[AB^*]/dt \approx 0$ as in Sect. 2.3), a Lindemann–Hinshelwood-type analysis leads to

$$d[AB]/dt = k_{\text{Ass}}[A][B] \quad (11)$$

$$d[C]/dt = d[D]/dt = k_{\text{CA}}[A][B] \quad (12)$$

$$d[A]/dt = -(k_{\text{Ass}} + k_{\text{CA}})[A][B]. \quad (13)$$

The rate constants for association (k_{Ass}) and for chemical activation leading to product formation (k_{CA}) then are given by

$$k_{\text{Ass}} = k_1 k_2 [M] / (k_{-1} + k_2 [M] + k_5) \quad (14)$$

$$k_{\text{CA}} = k_1 k_5 / (k_{-1} + k_2 [M] + k_5). \quad (15)$$

Note that k_{Ass} and k_{CA} are dependent on the nature and concentration of the third body M , in addition to their temperature dependence. In reality, as for combination and dissociation reactions, the given expressions for k_{Ass} and k_{CA} have to be extended by suitable broadening factors F to account for the multistep character of processes (2) and the energy and angular momentum dependences of processes (1), (–1) and (5). These broadening factors, however, generally

differ for k_{Ass} and k_{CA} : also they generally differ from those of simple combination reactions described in Sect. 2.3. One should note that association and chemical activation here are coupled such that their joint treatment is complicated. Some simplification is reached when the processes first are treated separately and the coupling is introduced at the end (Troé, 2015). The corresponding rate constants of the separated processes are denoted by k_{Ass}^* and k_{CA}^* and are given by

$$k_{\text{Ass}}^* = k_1 k_2 [M] / (k_{-1} + k_2 [M]) \quad (16)$$

and

$$k_{\text{CA}}^* = k_1 k_5 / (k_2 [M] + k_5). \quad (17)$$

k_{Ass}^* then corresponds to the rate constant of a combination reaction described in Sect. 2.3 and has a broadening factor $F_{\text{Ass}}^*(x^*)$. k_{CA}^* has to be treated in a different way and is expressed in the form

$$k_{\text{CA}}^* = k_{\text{Ass},\infty} [1 / (1 + x^*)] F_{\text{CA}}^*(x^*), \quad (18)$$

with $x^* = k_{\text{Ass},\infty} [M] / k_{\text{CA},\infty}^*$ and a broadening factor $F_{\text{CA}}^*(x)$ (Stewart et al., 1989). The latter factor is generally larger than $F_{\text{Ass}}^*(x^*)$ (Troé, 2015). The rate parameters $k_{\text{CA},0}^*$ and $k_{\text{CA},\infty}^*$ depend on the molecular parameters and can be calculated theoretically or fitted experimentally (after the coupling between association and chemical activation has been accounted for). In practice one may try to represent the rate constants in the form of rate constants of separated processes k_{Ass}^* and k_{CA}^* . Coupling these rate constants then leads to a full representation of the rate constants in terms of the six rate parameters $k_{\text{Ass},0}$, $k_{\text{Ass},\infty}$, $F_{\text{Ass},c}$, $k_{\text{CA},0}$, $k_{\text{CA},\infty}$ and $F_{\text{CA},c}$. If one neglects the coupling and fits these parameters directly from the experiments (Miller and Klippenstein, 2001), however, one has to be aware of the fact that the values obtained do not correspond to those of separated, single-channel, association and chemical activation processes (for more details, see Troé, 2015).

As a consequence of the multistep character of complex-forming bimolecular reactions, a variety of temperature and pressure dependences of k_{Ass} and k_{CA} are observed. The low-pressure limit of the total rate constants $k_{\text{tot}} = k_{\text{Ass}} + k_{\text{CA}}$, i.e. $k_{\text{tot},0} = k_{\text{CA},0} = k_1 k_5 / (k_{-1} + k_5)$, because of different energy and angular momentum dependences of the specific rate constants k_1 , k_{-1} and k_5 , may increase or decrease with temperature, the latter with the possibility of a change with an increase above a certain temperature. k_{tot} , as given above, may increase with pressure from $k_{\text{CA},0}$ to k_1 , with $M = \text{H}_2\text{O}$ often being a particularly efficient third body in the pressure-dependent range. The pressure dependence generally becomes less apparent with increasing temperature. Finally, the further fate of an addition product AB is of importance. It may be collisionally reactivated to energies where $k_5 \gg k_{-1}$, such that formation of $C + D$ is enhanced (in comparison to energies where $k_5 \ll k_{-1}$). There is also the possibility

that $A-M$ (or $B-M$) complexes are formed which react in a chaperon mechanism with B (or A) and then form products. $M = \text{H}_2\text{O}$ here may be particularly efficient. Without detailed theoretical analysis, in general, it will be difficult to disentangle the intrinsic mechanism. Therefore, reference to theoretical work is given for selected reactions.

2.5 Photochemical reactions

The data sheets begin with a list of feasible primary photochemical processes for wavelengths usually down to 185 nm, along with the corresponding enthalpy changes at 0 K where possible or alternatively at 298 K. Calculated threshold wavelengths corresponding to these enthalpy changes are also listed, bearing in mind that the values calculated from the enthalpy changes at 298 K are not true “threshold values”. This is followed by tables which summarize the available experimental data for (i) absorption cross sections and (ii) quantum yields. These data are supplemented by a series of comments. The next table lists the preferred absorption cross section data and the preferred quantum yields at appropriate wavelength intervals. For absorption cross sections, the intervals are usually 1, 5 or 10 nm. Any temperature dependence of the absorption cross sections is also given where possible. The aim in presenting these preferred data is to provide a basis for calculating atmospheric photolysis rates. For absorption continua, the temperature dependence is often represented by Sulzer–Wieland-type expressions (Astholz et al., 1981). Alternatively a simple empirical expression of the form $\log_{10}(\sigma_{T_1}/\sigma_{T_2}) = B^*(T_1 - T_2)$ is used. The comments again describe how the preferred data were selected and include other relevant points. The photochemical data sheets are concluded with a list of references.

2.6 Conventions concerning absorption cross sections

These are presented in the data sheets as “absorption cross sections per molecule, base e .” They are defined according to the following equation:

$$I/I_0 = \exp(-\sigma [N]l), \quad (19)$$

where I_0 and I are the incident and transmitted light intensities, $[N]$ is the number concentration of absorber (expressed in molecule cm^{-3}), l is the path length (expressed in cm) and σ is the absorption cross section (units of $\text{cm}^2 \text{ molecule}^{-1}$). Note that “molecule” is not a unit recognized by IUPAC but is included here for clarity. Other definitions and units are frequently quoted. The closely related quantities “absorption coefficient” and “extinction coefficient” are often used, but care must be taken to avoid confusion in their definition; see Calvert (1990) for definitions and discussion. It is always necessary to know the units of concentration and of path length and the type of logarithm (base e or base 10) corresponding to the definition. The decadic molar absorption

coefficient, ε , is often quoted, particularly in the older literature, and is defined as

$$\varepsilon = \{1/([A]l)\}\log_{10}(I_0/I), \quad (20)$$

where $[A]$ is the concentration of the absorber expressed in units of moles per cubic decimetre (moles dm^{-3}). While ε is often called an extinction coefficient, the term “extinction” should more properly be used for the sum of absorption and scattering. To convert from ε (base 10, units of $\text{dm}^3 \text{mol}^{-1} \text{cm}^{-1}$) to σ (base e , units of $\text{cm}^2 \text{molecule}^{-1}$), multiply it by 3.82×10^{-20} .

2.7 Assignment of uncertainties

Under the heading “reliability,” estimates have been made of the absolute accuracies of the preferred values of k at 298 K and of the preferred values of E/R over the quoted temperature range. The accuracy of the preferred rate coefficient at 298 K is quoted as the term $\Delta \log k$, where $\Delta \log k = d$ and d is defined by the equation, $\log k = c \pm d$. This is equivalent to the statement that k is uncertain to a factor of f , where $d = \log f$. The accuracy of the preferred value of E/R is quoted as the term $\Delta(E/R)$, where $\Delta(E/R) = g$ and g is defined by the equation $E/R = h \pm g$. d and g are uncertainties corresponding approximately to 95 % confidence limits. For second-order rate coefficients listed in this evaluation, an estimate of the uncertainty at any given temperature within the recommended temperature range may be obtained from the equation:

$$\Delta \log k(T) = \Delta \log k(298 \text{ K}) + 0.4343\{\Delta E/R(1/T - 1/298 \text{ K})\}.$$

The assignment of these absolute uncertainties in k and E/R is our subjective assessment. They are not determined by a rigorous, statistical analysis of the database, which is generally too limited to permit such an analysis. Rather, the uncertainties are based on our knowledge of the techniques, the difficulties of the experimental measurements, the potential for systematic errors and the number of studies conducted and their agreement or lack thereof. Experience shows that for rate measurements of atomic and free radical reactions in the gas phase, the precision of the measurement, i.e. the reproducibility, is usually good. Thus, for single studies of a particular reaction involving one technique, standard deviations, or even 95 % confidence limits, of $\pm 10\%$ or less are frequently reported in the literature. However, when we compare data for the same reaction studied by more than one group of investigators and involving different techniques, the rate coefficients sometimes differ by a factor of 2 or even more. This can only mean that one or more of the studies has involved large systematic uncertainty, which is difficult to detect. The differences between various measurements could be due to multiple reasons, such as insufficient purity of compounds, unknown/unexpected impurities, wall adsorption and decomposition, insufficient time resolution for the

initial elementary step, opposing and parallel reactions or unexpected decomposition products from the primary product. This is hardly surprising since, unlike molecular reactions, it is not always possible to study atomic and free radical reactions in isolation, and consequently mechanistic and other difficulties frequently arise. On the whole, our assessment of uncertainty limits tends towards the cautious side. Thus, in the case where a rate coefficient has been measured by a single investigation using one particular technique and is unconfirmed by independent work, we typically suggest an uncertainty of a factor of 2.

In contrast to the usual situation for the rate coefficients of thermal reactions, where inter-comparison of results of a number of independent studies permits a realistic assessment of reliability, for many photochemical processes there is a scarcity of data. Thus, we do not feel justified at present in assigning uncertainty limits to the parameters reported for the photochemical reactions.

Appendix A: Nomenclature

A	absorption
API	atmospheric pressure ionization
AS	absorption spectroscopy
CCD	charge-coupled detector
CEAS	cavity-enhanced absorption spectroscopy
CIMS	chemical ionization mass spectroscopy/spectrometry
CL	chemiluminescence
CRDS	cavity ring-down spectroscopy
DF	discharge flow
EPR	electron paramagnetic resonance
<i>F</i>	flow system
FP	flash photolysis
FTIR	Fourier transform infrared
FTS	Fourier transform spectroscopy
GC	gas chromatography/gas chromatographic
HPLC	high-performance liquid chromatography
IBBCEAS	incoherent broadband cavity enhanced absorption spectroscopy
IR	infrared
LIF	laser-induced fluorescence
LMR	laser magnetic resonance
LP	laser photolysis
MM	molecular modulation
MS	mass spectrometry/mass spectrometric
<i>P</i>	steady-state photolysis
PLP	pulsed laser photolysis
PR	pulse radiolysis
RA	resonance absorption
RF	resonance fluorescence
RR	relative rate
<i>S</i>	static system
TDLS	tunable diode laser spectroscopy
ToF	time of flight
UV	ultraviolet
UVA	ultraviolet absorption
VUVA	vacuum ultraviolet absorption

Data availability. All relevant data and supporting information have been provided in the Supplement. The detailed reaction data sheets are also available on the IUPAC Task Group on Atmospheric Chemical Kinetics Data Evaluation website at <http://iupac.pole-ether.fr/> (IUPAC, 2021).

Supplement. The supplement related to this article is available online at: <https://doi.org/10.5194/acp-21-4797-2021-supplement>.

Author contributions. All authors defined the scope of the work. AM, TJW, JNC, MEJ and RAC developed and drafted the data sheets and manuscript. All authors reviewed, refined and revised the manuscript and data sheets.

Competing interests. The authors declare that they have no conflict of interest.

Acknowledgements. The chairman and members of the task group wish to express their appreciation to IUPAC for the help which facilitated the preparation of this evaluation. We also acknowledge support from the following organizations: EU Framework Program 6 and 7 and Horizon 2020, the UK Natural Environmental Research Council, the Swiss National Science Foundation, the Centre National de la Recherche Scientifique-Institut National des Sciences de l'Univers (CNRS-INSU), Orléans University and Observatoire des Sciences de l'Univers en région Centre (OSUC). We thank Cathy Boone and Phuong Nguyen for constructing, developing and maintaining the website.

Review statement. This paper was edited by Ulrich Pöschl and reviewed by Cornelius Zetzsch and Geert Moortgat and three anonymous referees.

References

- Ammann, M., Cox, R. A., Crowley, J. N., Jenkin, M. E., Mellouki, A., Rossi, M. J., Troe, J., and Wallington, T. J.: Evaluated kinetic and photochemical data for atmospheric chemistry: Volume VI – heterogeneous reactions with liquid substrates, *Atmos. Chem. Phys.*, 13, 8045–8228, <https://doi.org/10.5194/acp-13-8045-2013>, 2013.
- Astholz, D. C., Brouwer, L., and Troe, J.: High-temperature ultraviolet-absorption spectra of polyatomic molecules in shock waves, *Ber. Bunsen. Phys. Chem.*, 85, 559–564, 1981.
- Atkinson, R., Baulch, D. L., Cox, R. A., Hampson Jr., R. F., Kerr, J. A., and Troe, J.: Evaluated kinetic and photochemical data for atmospheric chemistry: Supplement III, IUPAC Subcommittee on Gas Kinetic Data Evaluation for Atmospheric Chemistry, *J. Phys. Chem. Ref. Data*, 18, 881–1097, 1989.
- Atkinson, R., Baulch, D. L., Cox, R. A., Hampson Jr., R. F., Kerr, J. A., and Troe, J.: Evaluated kinetic and photochemical data for atmospheric chemistry: Supplement IV, IUPAC Subcommittee on Gas Kinetic Data Evaluation for Atmospheric Chemistry, *J. Phys. Chem. Ref. Data*, 21, 1125–1568, 1992.
- Atkinson, R., Baulch, D. L., Cox, R. A., Hampson Jr., R. F., Kerr, J. A., Rossi, M. J., and Troe, J.: Evaluated kinetic, photochemical, and heterogeneous data for atmospheric chemistry: Supplement V, IUPAC Subcommittee on Gas Kinetic Data Evaluation for Atmospheric Chemistry, *J. Phys. Chem. Ref. Data*, 26, 521–1011, 1997a.
- Atkinson, R., Baulch, D. L., Cox, R. A., Hampson Jr., R. F., Kerr, J. A., Rossi, M. J., and Troe, J.: Evaluated kinetic and photochemical data for atmospheric chemistry: Supplement VI, IUPAC Subcommittee on Gas Kinetic Data Evaluation for Atmospheric Chemistry, *J. Phys. Chem. Ref. Data*, 26, 1329–1499, 1997b.
- Atkinson, R., Baulch, D. L., Cox, R. A., Hampson Jr., R. F., Kerr, J. A., Rossi, M. J., and Troe, J.: Evaluated kinetic and photochemical data for atmospheric chemistry: Supplement VII, IUPAC Subcommittee on Gas Kinetic Data Evaluation for Atmospheric Chemistry, *J. Phys. Chem. Ref. Data*, 28, 191–393, 1999.
- Atkinson, R., Baulch, D. L., Cox, R. A., Hampson Jr., R. F., Kerr, J. A., Rossi, M. J., and Troe, J.: Evaluated kinetic and photochemical data for atmospheric chemistry, Supplement VIII, IUPAC Subcommittee on Gas Kinetic Data Evaluation for Atmospheric Chemistry, *J. Phys. Chem. Ref. Data*, 29, 167–266, 2000.
- Atkinson, R., Baulch, D. L., Cox, R. A., Crowley, J. N., Hampson, R. F., Hynes, R. G., Jenkin, M. E., Rossi, M. J., and Troe, J.: Evaluated kinetic and photochemical data for atmospheric chemistry: Volume I – gas phase reactions of O_x, HO_x, NO_x, and SO_x species, *Atmos. Chem. Phys.*, 4, 1461–1738, <https://doi.org/10.5194/acp-4-1461-2004>, 2004.
- Atkinson, R., Baulch, D. L., Cox, R. A., Crowley, J. N., Hampson, R. F., Hynes, R. G., Jenkin, M. E., Rossi, M. J., Troe, J., and IUPAC Subcommittee: Evaluated kinetic and photochemical data for atmospheric chemistry: Volume II – gas phase reactions of organic species, *Atmos. Chem. Phys.*, 6, 3625–4055, <https://doi.org/10.5194/acp-6-3625-2006>, 2006.
- Atkinson, R., Baulch, D. L., Cox, R. A., Crowley, J. N., Hampson, R. F., Hynes, R. G., Jenkin, M. E., Rossi, M. J., and Troe, J.: Evaluated kinetic and photochemical data for atmospheric chemistry: Volume III – gas phase reactions of inorganic halogens, *Atmos. Chem. Phys.*, 7, 981–1191, <https://doi.org/10.5194/acp-7-981-2007>, 2007.
- Atkinson, R., Baulch, D. L., Cox, R. A., Crowley, J. N., Hampson, R. F., Hynes, R. G., Jenkin, M. E., Rossi, M. J., Troe, J., and Wallington, T. J.: Evaluated kinetic and photochemical data for atmospheric chemistry: Volume IV – gas phase reactions of organic halogen species, *Atmos. Chem. Phys.*, 8, 4141–4496, <https://doi.org/10.5194/acp-8-4141-2008>, 2008.
- Baulch, D. L., Cox, R. A., Hampson Jr., R. F., Kerr, J. A., Troe, J., and Watson, R. T.: Evaluated kinetic and photochemical data for atmospheric chemistry, CODATA Task Group on Chemical Kinetics, *J. Phys. Chem. Ref. Data*, 9, 295–471, 1980.
- Baulch, D. L., Cox, R. A., Crutzen, P. J., Hampson Jr., R. F., Kerr, J. A., Troe, J., and Watson, R. T.: Evaluated kinetic and photochemical data for atmospheric chemistry: Supplement I, CODATA Task Group on Chemical Kinetics, *J. Phys. Chem. Ref. Data*, 11, 327–496, 1982.
- Baulch, D. L., Cox, R. A., Hampson Jr., R. F., Kerr, J. A., Troe, J., and Watson, R. T.: Evaluated kinetic and photochemical data

- for atmospheric chemistry: Supplement II, CODATA Task Group on Gas Phase Chemical Kinetics, *J. Phys. Chem. Ref. Data*, 13, 1259–1380, 1984.
- Calvert, J. G.: Glossary of atmospheric chemistry terms, *Pure Appl. Chem.*, 62, 2167–2219, 1990.
- Cobos, C. J. and Troe, J.: Prediction of reduced falloff curves for recombination reactions at low temperatures, *Z. Phys. Chem.*, 217, 1–14, 2003.
- Cox, R. A.: Evaluation of laboratory kinetics and photochemical data for atmospheric chemistry applications, *Chem. Soc. Rev.*, 41, 6231–6246, 2012.
- Cox, R. A., Ammann, M., Crowley, J. N., Herrmann, H., Jenkin, M. E., McNeill, V. F., Mellouki, A., Rossi, M. J., Troe, J., and Wallington, T. J.: IUPAC in the (real) clouds: 40 years of evaluating atmospheric chemistry data, *Chemistry International*, 40, 10–13, <https://doi.org/10.1515/ci-2018-0404>, 2018.
- Cox, R. A., Ammann, M., Crowley, J. N., Herrmann, H., Jenkin, M. E., McNeill, V. F., Mellouki, A., Troe, J., and Wallington, T. J.: Evaluated kinetic and photochemical data for atmospheric chemistry: Volume VII – Criegee intermediates, *Atmos. Chem. Phys.*, 20, 13497–13519, <https://doi.org/10.5194/acp-20-13497-2020>, 2020.
- Crowley, J. N., Ammann, M., Cox, R. A., Hynes, R. G., Jenkin, M. E., Mellouki, A., Rossi, M. J., Troe, J., and Wallington, T. J.: Evaluated kinetic and photochemical data for atmospheric chemistry: Volume V – heterogeneous reactions on solid substrates, *Atmos. Chem. Phys.*, 10, 9059–9223, <https://doi.org/10.5194/acp-10-9059-2010>, 2010.
- IUPAC, Task Group on Atmospheric Chemical Kinetic Data Evaluation: Evaluated kinetic data, available at: <http://iupac.pole-ether.fr/>, last access: 25 January 2021.
- Luther, K., Oum, K., and Troe, J.: The role of the radical-complex mechanism in the ozone recombination/dissociation reaction, *Phys. Chem. Chem. Phys.*, 7, 2764–2770, 2005.
- Miller, J. and Klippenstein, S. J.: The reaction between ethyl and molecular oxygen: Further analysis, *Int. J. Chem. Kinet.*, 33, 654–668, 2001.
- Oum, K., Sekiguchi, K., Luther, K., and Troe, J.: Observation of unique pressure effects in the combination reaction of benzyl radicals in the gas to liquid transition region, *Phys. Chem. Chem. Phys.*, 5, 2931–2933, 2003.
- Stewart, P. H., Larson, C. W., and Golden, D. M.: Pressure and temperature dependence of reactions proceeding via a bound complex, 2. An application to $2\text{CH}_3 \rightarrow \text{C}_2\text{H}_6 + \text{H}$, *Combust. Flame*, 75, 25–31, 1989.
- Teplukhin, A. and Babikov, D.: A full-dimensional model of ozone forming reaction: the absolute value of the recombination rate coefficient, its pressure and temperature dependencies, *Phys. Chem. Chem. Phys.*, 18, 19194–19206, 2016.
- Troe, J.: Theory of thermal unimolecular reactions in the fall-off range, I. Strong collision rate constants, *Ber. Bunsen. Phys. Chem.*, 87, 161–169, 1983.
- Troe, J.: Predictive possibilities of unimolecular rate theory, *J. Phys. Chem.*, 83, 114–126, 1979.
- Troe, J.: Simplified representation of partial and total rate constants of complex-forming bimolecular reactions, *J. Phys. Chem. A*, 119, 12159–12165, 2015.
- Troe, J. and Ushakov, V. G.: Revisiting falloff curves of thermal unimolecular reactions, *J. Chem. Phys.*, 135, 054304, <https://doi.org/10.1063/1.3615542>, 2011.
- Troe, J. and Ushakov, V. G.: Representation of “Broad” Falloff Curves for Dissociation and Recombination Reactions, *Z. Phys. Chem.*, 228, 1–10, 2014.